



**Queensland University of Technology**  
Brisbane Australia

This is the author's version of a work that was submitted/accepted for publication in the following source:

Buttsworth, David, Jacobs, Peter, Potter, Daniel, Mudford, Neil, D'Souza, Mary, Eichmann, Tory, Jenniskens, Peter, McIntyre, Tim, Jokic, Michael, Jacobs, Carolyn, [Upcroft, Ben](#), Khan, Razmi, Porat, Hadas, Neely, Andrew, & Lohle, Stefan (2011) Super-orbital re-entry in Australia : laboratory measurement, simulation and flight observation. In *28th International Symposium on Shock Waves*, 17 - 22 July 2011, University of Manchester, Manchester.

This file was downloaded from: <http://eprints.qut.edu.au/43726/>

**© Copyright 2011 [please consult the authors]**

**Notice:** *Changes introduced as a result of publishing processes such as copy-editing and formatting may not be reflected in this document. For a definitive version of this work, please refer to the published source:*

# Super-orbital Re-entry in Australia – laboratory measurement, simulation and flight observation

David Buttsworth<sup>1</sup>, Peter Jacobs<sup>2</sup>, Daniel Potter<sup>2</sup>, Neil Mudford<sup>3</sup>, Mary D'Souza<sup>2</sup>, Troy Eichmann<sup>2</sup>, Peter Jenniskens<sup>4</sup>, Tim McIntyre<sup>2</sup>, Michael Jokic<sup>1</sup>, Carolyn Jacobs<sup>2</sup>, Ben Upcroft<sup>5</sup>, Razmi Khan<sup>2</sup>, Hadas Porat<sup>2</sup>, Andrew Neely<sup>3</sup>, and Stefan Löhle<sup>6</sup>

## 1 Introduction

There are large uncertainties in the aerothermodynamic modelling of super-orbital re-entry which impact the design of spacecraft thermal protection systems (TPS). Aspects of the thermal environment of super-orbital re-entry flows can be simulated in the laboratory using arc- and plasma jet facilities and these devices are regularly used for TPS certification work [5]. Another laboratory device which is capable of simulating certain critical features of both the aero and thermal environment of super-orbital re-entry is the expansion tube, and three such facilities have been operating at the University of Queensland in recent years [10]. Despite some success, wind tunnel tests do not achieve full simulation, however, a virtually complete physical simulation of particular re-entry conditions can be obtained from dedicated flight testing, and the Apollo-era FIRE II flight experiment [2] is the premier example which still forms an important benchmark for modern simulations. Dedicated super-orbital flight testing is generally considered too expensive today, and there is a reluctance to incorporate substantial instrumentation for aerothermal diagnostics into existing missions since it may compromise primary mission objectives. An alternative approach to on-board flight measurements, with demonstrated success particularly in the 'Stardust' sample return mission, is remote observation of spectral emissions from the capsule and shock layer [8].

JAXA's 'Hayabusa' sample return capsule provides a recent super-orbital re-entry example through which we illustrate contributions in three areas: (1) physical simulation of super-orbital re-entry conditions in the laboratory; (2) computational simulation of such flows; and (3) remote acquisition of optical emissions from a super-orbital re-entry event.

---

*1. University of Southern Queensland, Toowoomba, Australia · 2. The University of Queensland, Brisbane, Australia · 3. University of New South Wales at ADFA, Canberra, Australia · 4. SETI Institute, California, USA · 5. Queensland University of Technology, Brisbane, Australia · 6. IRS, University of Stuttgart, Germany*

## 2 Laboratory Measurement

The majority of super-orbital flow experimentation at the University of Queensland over the last 5 years has been performed in the X2 facility. Recently, experiments on a 1/10 scale model of the Hayabusa sample return capsule were performed for an equivalent re-entry flight speed of 9.71 km/s. The nose radius of the models tested in the X2 facility was  $R = 20$  mm. Steel models, both with and without epoxy coatings on the forebody were tested. The useful test flow duration in X2 at this condition is about  $150 \mu\text{s}$ . Due to the heat transfer from the X2 flow, within tens of microseconds the epoxy surface begins to thermally degrade, emitting water vapour and hydrocarbon compounds into the shock layer. Details of the epoxy-coating method and these experiments are presented elsewhere [3, 1], but illustrative results are presented in Figs. 1 and 2.

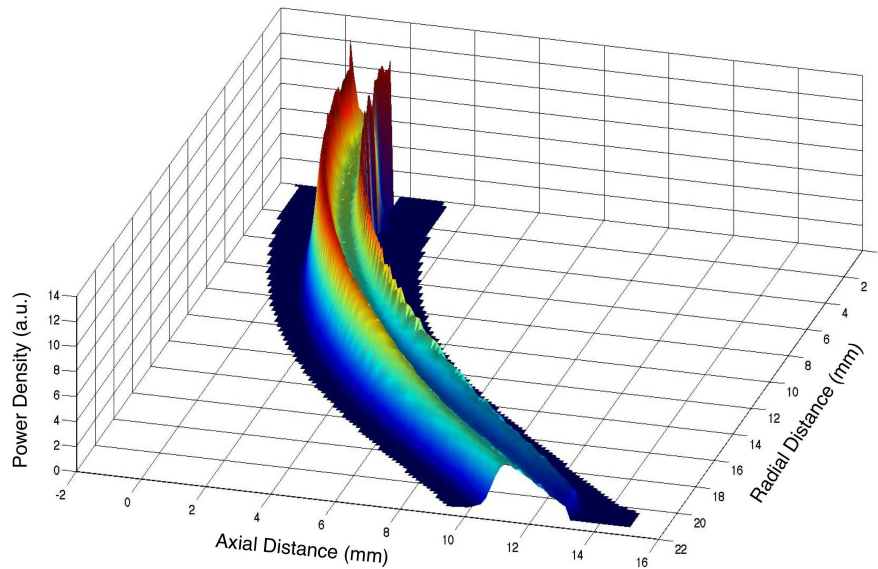


**Fig. 1** Emissions from the shock layer on an epoxy-coated subscale Hayabusa model which was tested in the X2 facility at a flow speed of 9.12 km/s. Data recorded on the HPV-1 high speed camera and analysed using the inverse Abel transform. Origin of the spatial axes is the intersection of the stagnation streamline and the normal shock. Figure taken from [1].

Figure 1 represents the shock layer emissions detected using the Shimadzu HPV-1 high speed camera for an epoxy-coated model. In this representation, the general direction of the flow is from left to right and two ridges in the shock layer emissions are apparent. The left-most ridge arises because of the nonequilibrium radiation which is established immediately behind the shock front. The second ridge corresponds to a luminous zone adjacent to the surface of the Hayabusa model which

occurs due to the epoxy coating – it is not observed on HPV-1 images for models without the epoxy coating.

Results in Fig. 2 were obtained using an Acton Research Spectra Pro 2300I spectrograph coupled to a Princeton Instruments PI-Max intensified CCD camera. The field of view of the spectrograph was a narrow strip, approximately 3.9 mm long which included the stagnation streamline. Figure 2 demonstrates the effect of the epoxy coating relative to the steel surface case – substantially higher emissions within the CN manifolds and emissions within the C<sub>2</sub> Swan bands are observed in the case of the epoxy-coated models.

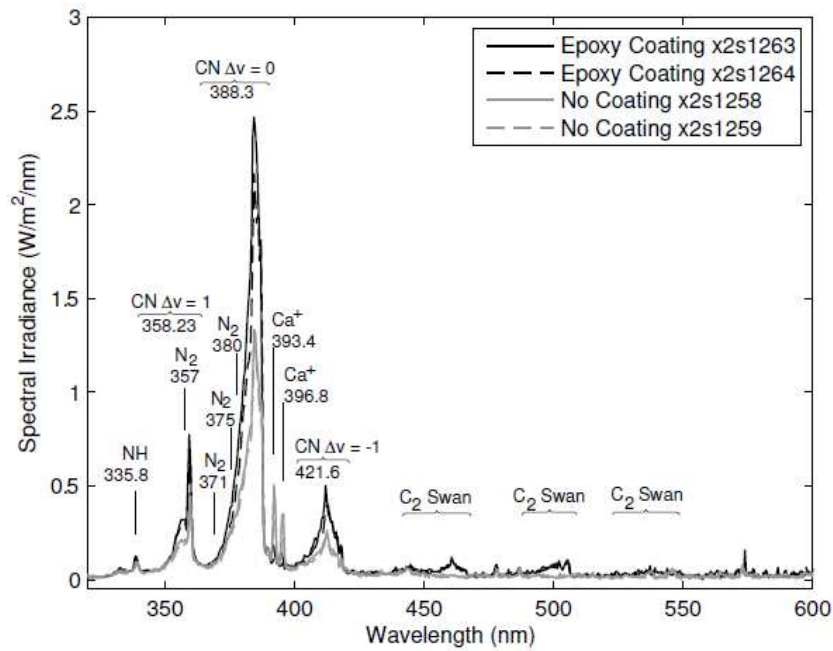


**Fig. 2** Spectral emissions from within the shock layer close to the surface of an epoxy-coated subscale Hayabusa model which was tested in the X2 facility at a flow speed of 9.12 km/s. Figure taken from [1].

### 3 Computational Simulation

Simulations of expansion tube operation are necessary because a complete set of test flow properties cannot be obtained directly from facility measurements alone. A hybrid approach which combines time-resolved one-dimensional control mass simulations (using ‘L1d’) with time-resolved axisymmetric control volume simula-

tions (using ‘Eilmer3’) has been used to deduce flow conditions for the Hayabusa experiments outlined in Section 2. L1d is an efficient tool for accurately simulating the free-piston compression and unsteady wave and flow processes with finite rate chemistry for conditions where the tube boundary layers are thin. For conditions in the acceleration tube and nozzle where viscous effects are strongly coupled to the unsteady wave and flow processes, Eilmer3 is the preferred tool because L1d forcibly merges the core and boundary layer and all viscous interactions such as heat transfer at the tube wall directly affect the core flow conditions. Details of the L1d and Eilmer3 simulation tools are presented elsewhere [7, 6]. Simulation of the X2 facility for the present operating condition is described in [11], and these simulations differ somewhat from earlier work reported in [1]. Selected flow parameters from the most recent simulations [11] are reported in Table 1.

**Table 1** Estimated free stream conditions generated in the X2 facility for the subscale Hayabusa experiments, from [11].

$u_\infty$ (km/s)	$T$ (K)	$T_v$ (K)	$\rho_\infty$ (kg/m <sup>3</sup> )	$u_{\text{equiv}}$ (km/s)
9.12	1070	1200	$1.73 \times 10^{-3}$	9.71
Mole Fractions ( $> 1 \times 10^{-6}$ ): N <sub>2</sub> : $6.27 \times 10^{-1}$ O <sub>2</sub> : $5.75 \times 10^{-3}$ NO: $2.18 \times 10^{-4}$ NO <sup>+</sup> : $7.24 \times 10^{-5}$ N: $3.63 \times 10^{-2}$ O: $3.30 \times 10^{-1}$ e <sup>-</sup> : $7.24 \times 10^{-5}$				

Inviscid simulations without radiative exchange for the steady flow around two spheres – one with radius  $R = 20$  mm (denoted ‘X2’), the other with  $R = 200$  mm (denoted ‘flight’) – were also performed using Eilmer3 [6]. Figure 3 shows the variation of density and  $N_2^+$  along the row of cells closest to the stagnation streamline for both conditions. The difference in the normalised shock stand-off distance –  $x/R \approx 0.052$  for ‘flight’ and  $0.057$  for ‘X2’ – arises because of the shock layer chemistry. For the simulations of the ‘flight’ conditions, the nonequilibrium region (where the  $N_2^+$  mass fraction varies rapidly) represents a small fraction of the shock layer thickness, whereas for the ‘X2’ simulations, the nonequilibrium region (and the region of relatively low shock layer density) is on the order of the shock layer thickness. The total enthalpies for the flight and X2 conditions are very similar: the capsule speed in the flight simulation was 9.69 km/s and the equivalent flight speed for the X2 conditions (based on the flow total enthalpy) was 9.71 km/s. However, the  $\rho L$  product in the case of the flight simulations was about 5 times larger than that of the X2 simulations; the laboratory experiments of Section 2 are subscale physical simulations of the re-entry event.

## 4 Flight Observation

The JAXA spacecraft, ‘Hayabusa’ re-entered the atmosphere above Australia late in the evening on the 13th of June 2010 at about 12 km/s, the fastest re-entry since

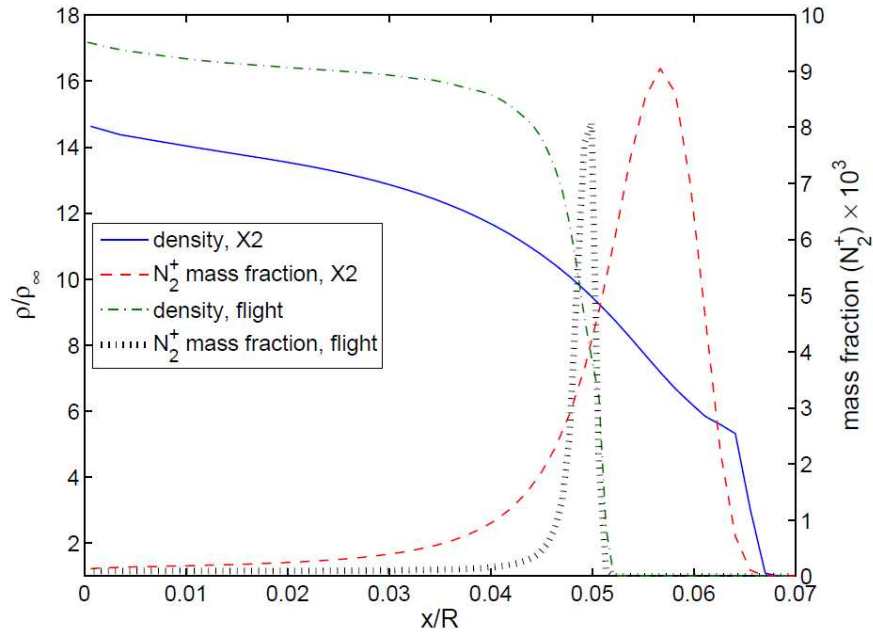


**Fig. 3** Results from computational simulations of spheres at super-orbital speeds. Variation of normalized density ( $\rho/\rho_\infty$ ) and  $N_2^+$  mass fraction close to the stagnation streamline plotted with normalized distance from the surface of the sphere ( $x/R$ ). Two cases are presented: ‘X2’ – sphere with radius  $R = 20$  mm with free stream conditions reported in Table 1, simulated using a  $60 \times 60$  array of cells; and ‘flight’ – sphere with radius  $R = 200$  mm travelling at 9.69 km/s and approximately 52 km altitude, simulated using a  $120 \times 120$  array of cells.

‘Stardust’ in 2006. Teams of researchers from the University of Queensland, the University of Southern Queensland, and the University of New South Wales at ADFA were positioned at Tarcoola and Coober Pedy for ground-based observations of the re-entry, and airborne observations were also made using an instrument on board the NASA DC-8 platform. A significant body of spectral data in the range 450 to 900 nm was acquired from the Tarcoola site using a semi-autonomous visual system developed for the event and this work is reported in a separate publication [4].

The configuration of the ‘AUS’ instrument (Australian Ultraviolet Spectrometer) which was used on the DC-8 platform is illustrated in Fig. 4. The instrument was mounted at station 610 (inches from the nose) in the DC-8, and at this station, a quartz window was fitted to enable acquisition of emission signatures in the near UV region. The AUS instrument consisted of a 45 degree fused silica prism positioned ahead of a 1200 lines/mm fused silica grating. An offset of approximately 10 degrees was applied to the prism to achieve a centre wavelength of about 375 nm on the intensified CCD array, as illustrated in Fig. 4. The 105 mm lens used in the AUS

device had colour correction between 250 and 650 nm and an f/4.5 aperture and was manufactured by Jenoptik.

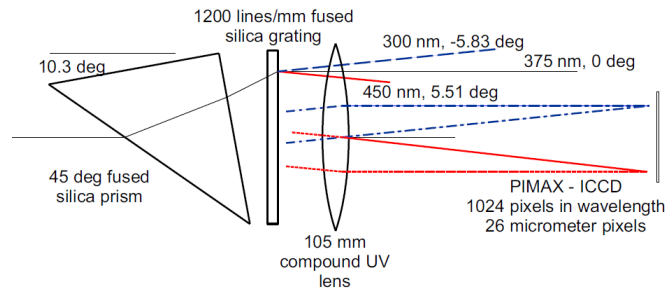


**Fig. 4** Optical arrangement of the Australian Ultraviolet Spectrometer ('AUS' Instrument) used on the DC-8 airborne observation laboratory for the Hayabusa re-entry observation.

The intensified CCD system in the AUS instrument has 1024 x 256 pixels (Princeton Instruments, PI-Max). The 1024 pixels were aligned in the vertical direction – the direction of the wavelength dispersion giving a resolution of 0.187 nm/pixel. The spectrometer field of view in the direction of the 256 pixels was approximately 3.6 degrees. A wide field of view video camera with good performance at low light levels was co-aligned with the spectrometer to facilitate manual tracking which was achieved by displaying the video signal on a headset display with cross-hairs.

A representative frame from the AUS instrument recorded at approximately 2 seconds after the peak in total (convective plus radiative) heating calculated to have been experienced by the Hayabusa capsule is presented in Fig. 5a. At this trajectory point, the estimated speed and altitude of the capsule are 9.69 km/s and 52 km respectively. During re-entry, the capsule was followed closely by the main bus, which disintegrated and was substantially brighter than the capsule itself. The proximity of the capsule and bus and the brightness of the bus made it difficult to distinguish the capsule emission signature from that of the bus for certain times leading up to peak heating. Nevertheless, capsule emission spectra were successfully acquired throughout the re-entry event using the AUS instrument.

The AUS instrument was calibrated at the NASA Ames Research Center post-flight using both an integrating sphere and a deuterium lamp with a wavelength reference provided by a mercury lamp. The counts on the CCD array were summed over the capsule region in the spatial direction (the vertical direction as presented in of Fig. 5a) and the background level was removed, giving the net counts from the capsule as a function of wavelength. Figure 5b was obtained by multiplying the net counts by the instrument calibration at each corresponding wavelength value.

Results in Fig. 5 show emissions from a variety of molecular and atomic species superimposed on the continuum emissions from the capsule surface. In this figure continuum emission is fitted using a Planck radiation curve with a temperature of

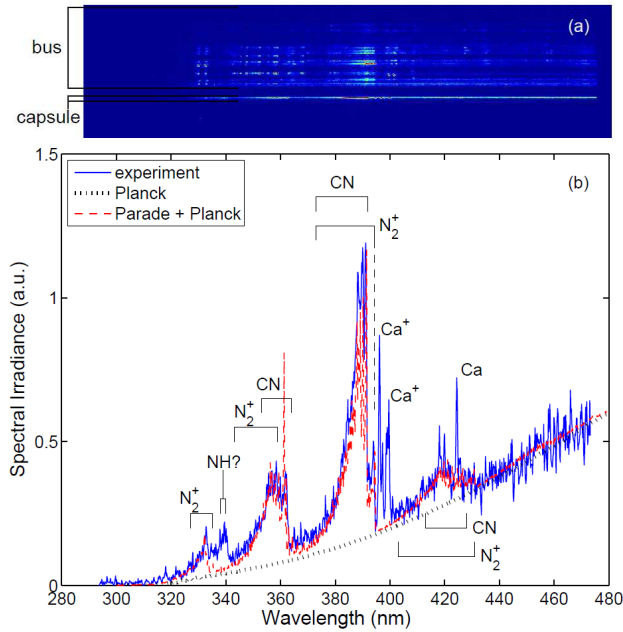


**Fig. 5** AUS instrument results acquired from the DC-8 aircraft at 13:52:22.40 (UTC) corresponding to approximately 2 seconds after the time of peak heating. Part (a): CCD image (false colour) from the AUS instrument illustrating the region of the Hayabusa capsule and the disintegrating bus. Part (b): spectral irradiance.

3254 K (based on data from two ground-based instruments [9]) after scaling with the estimated atmospheric transmission between the capsule and the DC-8. The molecular radiation has been simulated using the PARADE software [12] based on a manual selection of translational, vibrational, rotational, and electronic temperatures between the values of 5000 and 10000 K in order to fit the experimental data. The principal species contributing to observed molecular radiation are  $N_2$ ,  $N_2^+$  and CN. Contributions from NH have not yet been clearly identified. Carbon is a major element of Hayabusa's carbon phenolic ablator TPS so CN is expected to be generated primarily through the combination of dissociated nitrogen in the high temperature shock layer air and ablation products from the heat shield. Calcium lines (Ca and  $Ca^+$ ) are also apparent (Fig. 5) and aluminium can also be observed between the two  $Ca^+$  lines.

Contributions from  $N_2^+$  can be observed in Fig. 5, but  $N_2^+$  emissions did not feature in the laboratory result presented in Fig. 2. The emission spectra obtained from the Hayabusa re-entry represent an integration of the emission from the capsule and surrounding flow field. For the flight observation, each CCD pixel could receive emissions from an area of about  $50 \times 50$  m at the range of the capsule so the  $N_2^+$  formed in the nonequilibrium region of the shock layer can be a strong contributor to the observed emissions. In contrast, laboratory experiments can resolve spatial

variations within the Hayabusa shock layer; the results of Fig. 2 were from a location 0.15 mm ahead of the stagnation point, within the simulated ablation layer.

## 5 Conclusion

Substantial sets of super-orbital re-entry data have been obtained through laboratory experimentation using the X2 expansion tube facility and remote observation of the Hayabusa capsule's atmospheric descent. Computational tools suitable for simulating the super-orbital flows of the X2 facility and atmospheric re-entry have also been established recently. We expect that a more complete understanding of these complex flows can be achieved by employing these computational tools to analyse laboratory measurements in parallel with the flight data so we are proceeding in this direction.

## Acknowledgement

We would like acknowledge the Australian Research Council for support through the ARC Discovery program, the University of Queensland and the University of Southern Queensland for travel support for the Hayabusa observation mission, and computing support provided by the Queensland Smart State Research Facilities Fund and the UQ High Performance Computing Unit. We thank NASA for the invitation to participate in the airborne observation mission, Prof Richard Morgan for assistance with AUS instrument configuration, calibration and especially his accurate capsule targetting, Dr Michael Winter for assistance with instrument calibrations, and Dr Tetsuya Yamada of JAXA for facilitating the appointment of Hayabusa observers to the Hayabusa Joint Science Team.

## References

1. D R Buttsworth, M D'Souza, D Potter, T Eichmann, N Mudford, M McGilvray, T J McIntyre, P Jacobs, and R Morgan. Expansion tunnel radiation experiments to support hayabusa re-entry observations. In *48th AIAA Aerospace Sciences Meeting*, AIAA Paper 2010-634, Orlando, Florida, 4 – 7 January 2010.
2. D L Cauchon. Radiative heating results from FIRE II flight experiment at a re-entry velocity of 11.4 km/s. Technical Memorandum X-1402, NASA, 1967.
3. M G D'Souza, T N Eichmann, D F Potter, R G Morgan, T J McIntyre, P A Jacobs, and N R Mudford. Observation of an ablating surface in expansion tunnel flow. *AIAA Journal*, 48(7):1557–1560, 2010.
4. T. N. Eichmann, R. Khan, T. J. McIntyre, C. Jacobs, H. Porat, D. Buttsworth, and B. Upcroft. Radiometric temperature analysis of the hayabusa spacecraft re-entry. In *28th International Symposium on Shock Waves*, Manchester, UK, 17 – 22 July 2011.

5. G Herdrich, A Knapp, S Löhle, D Petkow, and S Fasoulas. Ground testing facilities and modeling tools: Research examples. In *27th AIAA Aerodynamic Measurement Technology and Ground Testing Conference*, AIAA Paper 2010-4339, Chicago, Illinois, 28 June – 1 July 2010 2010.
6. P. A. Jacobs and R. J. Gollan. The Eilmer3 code: User guide and example book. Mechanical Engineering Report 2008/07, The University of Queensland, Brisbane, Australia, 2010.
7. P. A. Jacobs, R. J. Gollan, D. F. Potter, D. E. Gildfind, T. N. Eichmann, B. T. O’Flaherty, and D. R. Buttsworth. CFD tools for design and simulation of transient flows in hypersonic facilities. In O. Chazot and K. Bensassi, editors, *RTO-AVT-VKI Lecture Series 2010-AVT186 Aerothermodynamic Design, Review on Ground Testing and CFD.*, Belgium, March 2010. von Karman Institute for Fluid Dynamics.
8. D A Kontinos and M J Wright. Introduction: Atmospheric entry of the Stardust sample return capsule. *Journal of Spacecraft and Rockets*, 47(6):865–867, 2010.
9. S. Löhle, T. Marynowski, and A. Mezger. Spectroscopic analysis of the hayabusa re-entry using airborne and ground based equipment. In *7th European Aerothermodynamics Symposium on Space Vehicles*, Brugge, Belgium, 2011.
10. R. G. Morgan, T. J. McIntyre, D. R. Buttsworth, P. A. Jacobs, D. F. Potter, A. M. Brandis, R. J. Gollan, C. M. Jacobs, B. R. Capra, M. McGilvray, and T. N. Eichmann. Impulse facilities for the simulation of hypersonic radiating flows. In *38th Fluid Dynamics Conference and Exhibit*, pages Paper AIAA–2008–4270. American Institute of Astronautics and Aeronautics, June 2008.
11. D F Potter. Ph.D. dissertation, Department of Mechanical and Mining Engineering, University of Queensland, Brisbane, Australia, 2011.
12. A. J. Smith, A. Wood, J. Dubois, M. Fertig, and B. Pfeiffer. Plasma radiation database PA-RADE v2.2, Final Report Issue 3. TR28/96 Issue 3, ESTEC Contract 11148/94/NL/FG, October 2006.